Journal of Solid State Chemistry **144,** 277–286 (1999)
Article ID jssc.1998.8124, available online at http://www.idealibrary.com on IDEAL®

Crystal Chemistry of Defective Intermetallics with Empty Triangular Metalloid Channels: The New Phosphide $Zr_6Cr_{60}P_{39}$

C. Le Sénéchal,* V. Babizhets'ky,*,[1] S. Députier,* J. Y. Pivan,† and R. Guérin*,[2]

*Laboratoire de Chimie du Solide et Inorganique Moléculaire, UMR 6511, and †Laboratoire de Physicochimie Analytique, ENSC Rennes, CNRS, Campus de Beaulieu, Avenue du Général Leclerc, 35042 Rennes Cédex, France

Received July 14, 1998; in revised form November 20, 1998; accepted November 27, 1998

The ternary compound $ZrCr_{60}P_{39}$ has been synthesized by the tin flux method. It presents a hexagonal crystal structure [a = 21.413(2) Å, c = 3.354(1) Å], space group $P6_3/m$, with one formula per unit cell. The X-ray structure has been refined from three-dimensional single-crystal intensity data to a final R value of 0.053 (R_w = 0.056) for 451 reflections [$I > 2\sigma(I)$]. The resulting structure is of a new type and exhibits empty triangular phosphorus channels. This structure belongs to a new series of hexagonal defective compounds named direct series with a metal/nonmetal ratio slightly lower than 2, the first members of which are the compounds $Cr_{12}P_7$ and $Zr_2Cr_{30}P_{19}$. The structural relationships with the reverse series, including the ternaries $R_2Co_{12}P_7$ (R = rare earth element), $Yb_6Co_{30}P_{19}$, UCo_5Si_3, $U_6Co_{30}Si_{19}$, and $U_{10}Co_{51}Si_{33}$, are discussed in terms of metal vacancies and coordination polyhedra. Finally, a general crystal chemical rule has been established that permits prediction of the different members for the two series and their definition structurally in terms of lattice parameters and theoretical X-ray diffraction patterns. Moreover this rule gives for each member the number of empty triangular metalloid channels as well as the distribution of the different polyhedra occupied by the metal atoms (trigonal prisms, pyramids, tetrahedra).

Key Words: **intermetallics; crystal structure; defective phosphides; structural relationships.**

INTRODUCTION

We have recently reported on a new ternary phosphide $Zr_2Cr_{30}P_{19}$ which had been synthesized during our preliminary study of the Zr–Cr–P system (1). The X-ray single-crystal structure has demonstrated strong relationships with another defective ternary phosphide $Yb_6Co_{30}P_{19}$ (2). Both structures crystallize in hexagonal symmetry, space group P-6, with similar lattice parameters [a = 14.807(4) Å, c = 3.348(1) Å for the zirconium phosphide and a = 14.703(4) Å, c = 3.574(1) Å for the ytterbium compound] and the same phosphorus polyhedra (trigonal prisms, pyramids, tetrahedra, and triangles). The main structural difference is the way in which the different phosphorus sites are occupied by the metal atoms. Indeed, in the case of $Zr_2Cr_{30}P_{19}$, the zirconium atoms occupy 2 phosphorus trigonal prisms and the chromium atoms 21 phosphorus pyramids and nine phosphorus tetrahedra, and there are 6 empty triangular phosphorus sites. In the case of $Yb_6Co_{30}P_{19}$, the number of phosphorus sites is identical but the way in which they are occupied is different: six ytterbium atoms occupy 6 trigonal prisms, the cobalt atoms occupy 21 tetrahedra and 9 pyramids, and there are two empty triangular phosphorus sites. Moreover, it has been shown that the structural relationship between $Zr_2Cr_{30}P_{19}$ and $Yb_6Co_{30}P_{19}$, on one hand, and $Cr_{12}P_7$ (3) and $R_2Co_{12}P_7$ (4) (R = rare earth element), on the other hand, resulted from the same crystal chemical mechanism. Indeed, the binary $\square_2Cr_{12}P_7$ and the ternary $\square_6Zr_2Cr_{30}P_{19}$ are members of a series called direct series with formula $\square_{n(n+1)}R_{n(n-1)}T_{6(n^2+1)}X_{2(2n^2+1)+1}$. In the same way, the ternaries $R_2Co_{12}P_7$ and $Yb_6Co_{30}P_{19}$ are members of a series called reverse series with formula $\square_{n(n-1)}R_{n(n+1)}T_{6(n^2+1)}X_{2(2n^2+1)+1}$. For the two series, R, T, and X represent Zr (or a rare earth element), a 3d transition metal, and the metalloid, respectively, $\square$ is a metal vacancy, and n is an integer. The four compounds, mentioned above are the first members (n = 1, 2) of the two series.

During the investigation of the Zr–Cr–P system, we found a new ternary phase $Zr_6Cr_{60}P_{39}$ which crystallizes in hexagonal symmetry with the unit cell parameters a = 21.413(2) Å and c = 3.354(1) Å. The crystal structure was solved from single-crystal data. This new defective structure is the member n = 3 of the direct series and exhibits consequently strong relationships with that of the ternary silicide $U_{12}Co_{60}Si_{38}$ (5), term n = 3 of the reverse series. By extension, it has been possible to extrapolate structurally to other members of the two series ($n > 3$), almost not yet known, and to propose their hexagonal unit

[1] Permanent address: Analytical Chemistry Department, Ivan Franko L'viv State University, Ukraine.
[2] To whom correspondence should be addressed. Fax: 2–99–63–57–04. E-mail: roland.guerin@univ-rennesl.fr.

0022-4596/99 $30.00

cell parameters, their theoretical X-ray diffraction patterns, as well as the overall number and occupancy of metalloid sites (trigonal prisms, pyramids, tetrahedra, and triangles).

The aim of this paper is to present the structural features of the new phosphide $Zr_6Cr_{60}P_{39}$ and to define the general crystal chemical rule used to describe all the members of two series (direct and reverse) of defective compounds.

EXPERIMENTAL

The samples were prepared by the tin flux method. Starting materials were zirconium (purity higher than 97%) and chromium (>99.5%) as powders, ultrapure red phosphorus (> 99.99%) as ingots, and tin (> 99.99%) as granules. The elements, in the atomic ratio Zr:Cr:P:Sn = 3:13:9:75, were sealed in evacuated silica tubes, which were slowly heated to 1100°C and held at this temperature for 1 week. After slow cooling in air, the tin-rich matrix was dissolved in diluted hydrochloric acid. The samples appeared in the form of shiny black needles. Energy-dispersive analysis of these single crystals in a scanning electron microscope confirmed the presence of zirconium, chromium, and phosphorus as the only components. The X-ray powder pattern (monochromated Cu$K\alpha$ radiation) of the new phosphide $Zr_6Cr_{60}P_{39}$ was found to be very close to that of $Zr_2Cr_{30}P_{19}$. The hexagonal symmetry of $Zr_6Cr_{60}P_{39}$ was established from Weissenberg patterns with the Laüe group $6/m$. Single-crystal intensity data were collected at ambient temperature using a four-circle diffractometer (CAD-4, Enraf–Nonius) with graphite-monochromated Mo$K\alpha$ radiation. The unit cell parameters and orientation matrix resulted from least-squares refinement of 25 optimized reflections collected within the range $8° \leq \theta \leq 18°$. Crystal stability was monitored with six standard reflections whose intensities were controlled every hour; no crystal decay was detected during intensity collection. The data were corrected from Lorentz factors and polarization effects, and an absorption correction was performed using ψ-scan method. The experimental details are summarized in Table 1. Intensity data and structure calculations were performed with the structure program package MolEN (7) implemented on a Vax-Station 3100 computer.

The structure of $Zr_6Cr_{60}P_{39}$ was solved by direct methods using MULTAN 11/82 (8) and subsequent difference Fourier syntheses in the centrosymmetric space group $P6_3/m$. The initial steps of refinement permitted us to easily locate the 6 zirconium atoms, 54 chromium atoms, then successively 36 phosphorus atoms in 16 sets of positions (6*h*). At this stage, a difference synthesis showed peaks on the threefold axes, which were attributed unambiguously to two phosphorus atoms in position (2*c*). Another peak was found on the *c*-axis corresponding to the position (2*a*). This peak was attributed to only one phosphorus atom due to the small value of the *c* parameter (3.354 Å). Indeed, as usually found in the chemistry of phosphides and related compounds with metal/nonmetal ratios close to 2, the whole occupancy of position (2*a*) is not possible as this would result in a short P–P distance of 1.677 Å. One must have in mind that the shortest known P–P distances are about 2.20 Å, which correspond to the covalent diameter of phosphorus (9), and they occur only in very rich phosphorus compounds (10).

The disorder of the phosphorus atoms, located on the *c* axis, disturbed the surrounding chromium atoms which have to be split into two sets of half-filled positions (6*h*). Such a disorder of metal atoms, around the *c*-axis, is well known in hexagonal structures of M_2X intermetallics (M = metal, X = metalloid). Indeed, numerous examples of this metalloid disorder on the *c* axis coupled to that of the surrounding metal atoms can be found in the literature as,

TABLE 1
Crystal Data, Intensity Collection, and Refinement for $Zr_6Cr_{60}P_{39}$[a]

I. Crystal data	
Formula	$Zr_6Cr_{60}P_{39}$
Molecular weight (g mol^{-1})	4875
Crystal size (mm^3)	$0.20 \times 0.01 \times 0.01$
Crystal system	hexagonal
Space group	$P6_3/m$
a (Å)	21.413 (2)
c (Å)	3.354 (1)
V (Å^3)	1332.3 (3)
Z	1
Density (calc., g cm^{-3})	6.08
Linear absorption coefficient (mm^{-1})	13.66
II. Data collection	
Temperature	293 K
Wavelength	Mo$K\alpha$ radiation (λ = 0.71073 Å)
Scan method	ω-2θ
Scan width	1 + 0.35 tg θ
Data collected	$-30 < h < 0$, $0 < k < 30$, $0 < 1 < 4$
θ limits	1–35
Number of measured reflections	3097
Number of independent reflections	908 [$I > 1\sigma(I)$]
Number of reflections in refinement	451 [$I > 2\sigma(I)$]
III. Structure determination	
Structure solution	Direct methods and Fourier
Refinement	Full-matrix least-squares
Refined parameters	58
Ponderation factor	$\omega = 4F_0^2/[\sigma^2 (F_0^2) + (0.02F_0^2)^2]$
Unweighted R factor	0.053
Weighted R_ω factor	0.056
$(\Delta/\sigma)_{max}$	< 0.01
Extinction coefficient	3.7×10^{-8}
Min/max (eÅ^{-3})	− 1.4/3.2
S (all data)	1.28

[a] Atomic scattering factors from "International Tables for Crystallography (6).

for example, for crystal structures of $Cr_{12}P_7$ (3), $Rh_{12}As_7$ (11), $(La,Ce)_{12}Rh_{30}P_{21}$ (12), $La_6Rh_{32}P_{17}$ (13), $Ho_{20}Ni_{66}P_{43}$ (14). At this stage of refinement the number of independent reflections in the intensity data set [456 reflections with $I > 2\sigma(I)$] compared with the number of refined parameters (37 variables) did not permit suppression of the disorder mechanism on and around the c axis, by considering the noncentrosymmetric space group $P\bar{6}$. Most of the hexagonal structures reported today in phosphide chemistry with a metal/nonmetal ratio equal or close to 2 have been solved in the space group $P6_3/m$ or $P\bar{6}$ without significant structural differences. Indeed, the true space group is difficult to identify because the $00l$ reflections with $l = 2n + 1$, when present, are always very weak and are rejected from the intensity data set when applying the condition $I > 1\sigma(I)$.

The reliability factor was improved when isotropic thermal parameters were refined together with secondary extinction factors. As usually found in related structures, the isotropic thermal parameters were less than 1.2 Å^2, except for phosphorus atoms P7 and P8 on the threefold and sixfold axes and chromium atoms Cr10 and Cr11 around the c axis. Delocalization of the phosphorus atoms P7 and P8 in positions ($4f$) and ($4e$), with respective occupancy factors of 1/2 and 1/4, was tested without significant improvement. In fact, numerous examples with high values of isotropic thermal parameters for atoms in such a disposition are common in the literature (12–14).

The residual values R and R_w (0.053 and 0.056, respectively) were obtained for 58 variable parameters and 451 structure factors with $I > 2\sigma(I)$. A final difference Fourier synthesis did not reveal any significant electronic density peaks. Atomic positional and thermal coordinates are listed in Table 2 and selected interatomic distances in Table 3. Observed and calculated structure factors can be obtained on request from the authors.

STRUCTURAL DESCRIPTION

A projection on the (001) plane of the crystal structure of $Zr_6Cr_{60}P_{39}$ is shown in Fig. 1. The structure, which is of a new type in pnictide chemistry, is characterized by one set of zirconium atoms located in quite regular trigonal phosphorus prisms. The (ZrP_6) prisms, displayed around the threefold axes, are stacked on each other by common faces along the (001) direction, so as to develop infinite channels. Other infinite trigonal phosphorus channels are arranged six at a time in two sets, around the threefold axes of the unit cell. These channels consist of empty prisms which share common edges with the (ZrP_6) prisms.

As commonly found in the structures of the M_2X family compounds, the hexagonal framework, built up here by three CrP_4 tetrahedra and three CrP_5 pyramids, occurs around the origin of the unit cell. This framework is known to be the basis of the Fe_2P structure (15). Between the phosphorus channels (occupied prisms or vacant triangles) and the hexagonal framework, two types of intermediate structural domains are present that consist of chromium atoms occupying either pyramidal or tetrahedral phosphorus sites.

Taking into account the different phosphorus polyhedra, the compound $Zr_6Cr_{60}P_{39}$ can be expressed as $\square_{12}^{tr.}Zr_6^{pr.}Cr_{39}^{py.}Cr_{21}^{tet}P_{39}$ or $\square_{12}^{tr.}Zr_6^{pr.}(Cr_{36}^{py.}Cr_{18}^{tet.})_{int.dom.}(Cr_3^{py.}Cr_3^{Tet.})_{hex.fr.}P_{39}$ (relation 1), when considering the different domains in the structure. The abbreviations pr., tr., tet., and py. stand for prismatic, triangular, tetrahedral, and pyramidal phosphorus sites, respectively.

With the exception of the phosphorus atoms P7 and P8 located on the threefold and sixfold axes, which exhibit the usual tricapped trigonal prismatic metal coordination, all phosphorus atoms occupy bicapped trigonal metal prisms. That means that the metal defect in the compounds corresponds to triangular phosphorus vacancies (Fig. 1).

All the mean distances Zr–P (2.74 Å) and Cr–P (2.41 Å in pyramidal, 2.30 Å in tetrahedral coordination) found in the structure are in good agreement with similar distances, previously reported in numerous binary and ternary phosphides with a metal/nonmetal ratio equal or close to 2 and for similar coordination [for comparison see Ref. (1)]. These distances are in accordance with the sum of the covalent radius of phosphorus (1.10 Å) (9) and the metal radius of chromium or zirconium [1.28 or 1.60 Å in 12-coordination respectively (16)]. The length of the c axis

TABLE 2
Positional and Thermal Isotropic Coordinates of $Zr_6Cr_{60}P_{39}$ and Estimated Standard Deviations

Atom	x	y	z	B (Å^2)
Zr	0.5428(2)	0.8257(2)	0.25	0.85(4)
Cr1	0.6789(2)	0.1041(2)	0.75	0.45(8)
Cr2	0.5836(3)	0.2699(3)	0.25	1.06(9)
Cr3	0.5335(1)	0.0621(2)	0.75	0.56(8)
Cr4	0.8357(3)	0.0462(3)	0.25	0.81(7)
Cr5	0.3097(3)	0.9966(3)	0.75	0.77(9)
Cr6	0.2049(3)	0.5696(3)	0.25	0.56(8)
Cr7	0.1707(3)	0.2690(2)	0.25	0.65(8)
Cr8	0.3605(3)	0.2053(2)	0.25	0.90(9)
Cr9	0.4258(2)	0.0462(2)	0.25	0.45(8)
Cr10[a]	0.0623(5)	0.1240(5)	0.25	1.1(2)
Cr11[a]	0.9497(6)	0.9005(6)	0.75	1.8(2)
P1	0.6044(4)	0.4577(4)	0.25	0.3(1)
P2	0.4844(4)	0.2867(4)	0.25	0.6(1)
P3	0.3454(4)	0.0898(4)	0.25	0.6(1)
P4	0.7008(4)	0.7753(4)	0.25	0.4(1)
P5	0.1792(4)	0.0395(4)	0.25	1.2(2)
P6	0.5941(4)	0.0346(4)	0.25	0.7(1)
P7	1/3	2/3	0.25	2.5(4)
P8[a]	0	0	0.25	1.5(6)

[a] Occupancy factor 0.5.

TABLE 3
Main Interatomic Distances (Å) of $Zr_6Cr_{60}P_{39}$ (<3.35 Å)[a]

Zr–	2 P3	2.736	Cr6–	2 P1	2.420	P1–	1 Cr2	2.326
	2 P2	2.747		2 P2	2.426		1 Cr9	2.341
	2 P1	2.749		1 P7	2.484		2 Cr3	2.406
	2 Cr2	2.965		1 Cr3	2.728		2 Cr6	2.420
	2 Cr8	2.988		2 Cr2	2.743		2 Zr	2.749
	2 Cr9	2.990		1 Cr1	2.745		1 P6	3.109
				2 Cr2	2.762		1 P2	3.257
Cr1–	2 P6	2.371						
	2 P2	2.428	Cr7–	2 P5	2.383	P2–	1 Cr2	2.325
	1 P4	2.445		2 P3	2.413		1 Cr8	2.335
	2 Cr8	2.729		1 P4	2.449		2 Cr6	2.426
	1 Cr6	2.745		1 Cr5	2.720		2 Cr1	2.428
	1 Cr3	2.775		2 Cr8	2.723		2 Zr	2.747
	2 Cr5	2.838		1 Cr4	2.768		1 P6	3.130
	1 Cr9	2.859		1 Cr10	2.797		1 P1	3.257
				2 Cr4	2.856			
Cr2–	1 P2	2.325		1 Cr11	3.235	P3–	1 Cr8	2.330
	2 P7	2.326					1 Cr9	2.333
	1 P1	2.326	Cr8–	2 P4	2.291		2 Cr7	2.413
	2 Cr6	2.743		1 P3	2.330		2 Cr5	2.420
	2 Cr6	2.762		1 P2	2.335		2 Zr	2.736
	2 Cr2	2.790		2 Cr7	2.723		1 P4	3.157
	2 Zr	2.965		2 Cr1	2.729		1 P5	3.162
				1 Cr4	2.874			
Cr3–	2 P6	2.370		1 Cr5	2.879	P4–	2 Cr8	2.291
	2 P1	2.406		2 Zr	2.988		2 Cr4	2.374
	1 P6	2.468					2 Cr5	2.383
	1 Cr6	2.728	Cr9–	2 P6	2.292		1 Cr1	2.445
	2 Cr9	2.731		1 P3	2.333		1 Cr7	2.449
	1 Cr1	2.775		1 P1	2.341		1 P5	3.048
	2 Cr3	2.851		2 Cr3	2.731		1 P3	3.157
	1 Cr9	2.857		2 Cr5	2.735			
				1 Cr3	2.857	P5–	1 Cr10	2.365
Cr4–	2 P4	2.374		1 Cr1	2.859		2 Cr7	2.383
	2 P5	2.387		2 Zr	2.990		2 Cr4	2.387
	1 P5	2.408					1 Cr4	2.408
	1 Cr7	2.768	Cr10–	2 P5	2.236		2 Cr11	2.474
	1 Cr5	2.772		1 P8	2.300		1 P4	3.048
	1 Cr10	2.843		1 P5	2.365		1 P3	3.162
	2 Cr7	2.856		2 Cr4	2.646			
	1 Cr8	2.874		2 Cr11	2.689	P6–	2 Cr9	2.292
	2 Cr11	2.948		2 Cr11	2.702		2 Cr3	2.370
				1 Cr7	2.797		2 Cr1	2.371
Cr5–	2 P4	2.383		1 Cr4	2.843		1 Cr5	2.461
	2 P3	2.420					1 Cr3	2.468
	1 P6	2.461	Cr11–	1 P5	2.470		1 P1	3.109
	1 Cr7	2.720		2 P5	2.474		1 P2	3.130
	2 Cr9	2.735		2 P8	2.493			
	1 Cr4	2.772		2 Cr10	2.689	P7–	6 Cr2	2.326
	2 Cr1	2.838		2 Cr10	2.702		3 Cr6	2.484
	1 Cr8	2.879		2 Cr4	2.948			
				1 Cr4	2.988	P8–	3 Cr10	2.300
				2 Cr11	3.195		6 Cr11	2.493
				1 Cr7	3.235			

[a]SD are less than 9×10^{-3} Å for all distances.

(3.354 Å) does not allow for P–P bonds. On the contrary, numerous metal–metal bondings Zr–Zr, Zr–Cr, and Cr–Cr occur in the structure that results in a tridimensional metallic network.

DISCUSSION

The structure of $Zr_6Cr_{60}P_{39}$ is closely related to that of the ternary silicide of uranium and cobalt $U_6Co_{30}Si_{19}$, reported by Aksel'rud and co-workers (5). Indeed, the latter compound crystallizes in hexagonal symmetry, with unit cell constants $a = 21.14(1)$ Å and $c = 3.6933(4)$ Å close to those of $Zr_6Cr_{60}P_{39}$, with two formula units per cell. The crystal structure of this ternary silicide, i.e., $U_{12}Co_{60}Si_{38}$, given in projection on the (001) plane in Fig. 2, has been solved in the space group $P6_3/m$. Both structures $Zr_6Cr_{60}P_{39}$ and $U_{12}Co_{60}Si_{38}$ show a close network of metalloid atoms (P or Si occupying close atomic positions). The main difference arises from the absence of a silicon atom at the origin of the unit cell for the silicide.

Although the absence of silicon modifies the coordination scheme of cobalt atoms around the c axis, one can consider that the usual framework, found in hexagonal structures with space group $P6_3/m$ or P-6, is nevertheless maintained. It consists here of three $CoSi_3\square_2$ pyramids and three $CoSi_3\square$ tetrahedra. Hereafter in the text, to facilitate the discussion, it is better to consider that a silicon atom is present at the origin. Thereby the corresponding formula is written $U_{12}Co_{60}Si_{38+1}$. The two structures $Zr_6Cr_{60}P_{39}$ and $U_{12}Co_{60}Si_{38+1}$ differ from each other in the way the different metalloid sites are occupied. In the phosphide structure, the 6 filled channels correspond to ZrP_6 prisms and the 12 empty channels to triangular phosphorus vacancies. This result is inverted in the structure of the silicide. The prism↔triangle exchange results, in turn, in pyramid↔tetrahedron exchange so that the silicide structure can be written $U_{12}^{pr.}\square_6^{tr.}Co_{21}^{py.}Co_{39}^{tet.}Si_{38+1}$, with respect to that given for $Zr_6Cr_{60}P_{39}$.

Consequently this arrangement modifies, likely for steric reasons, the relative distribution of the transition metal atoms (Cr or Co) in the intermediate structural domains. Indeed, the numbers of occupied pyramids and tetrahedra, respectively 36 and 18 for $Zr_6Cr_{60}P_{39}$, become 18 and 36 in the case of $U_{12}Co_{60}Si_{38+1}$. The structural mechanism corresponding to the occupancy inversion of metalloid sites (prism↔empty triangle, pyramid↔tetrahedron) between both structures is the same as that previously described for the phosphides $Zr_2Cr_{30}P_{19}$ and $Yb_6Co_{30}P_{19}$ [see Introduction and Ref. (1)]. As a consequence, the developed formula of $U_{12}Co_{60}Si_{38+1}$, compared with relation (1), can be written $U_{12}^{pr.}\square_6^{tr.}(Co_{36}^{tet.}Co_{18}^{py.})_{int.dom.}(Co_3^{py.}Co_3^{tet.})_{hex.fr.}Si_{38+1}$.

It is obvious from structural considerations that the phosphides $Zr_2Cr_{30}P_{19}$ and $Zr_6Cr_{60}P_{39}$ are members of the same series called direct series, while the ternaries $Yb_6Co_{30}P_{19}$ [or isostructural $U_6Co_{30}Si_{18+1}$ (17)] and $U_{12}Co_{60}Si_{38+1}$ are members of another series called reverse series. These two series are not isopointal as defined by Parthé *et al.* (18) since the atomic positions in both series are not exactly the same. The general formula is $\square_{n(n+1)}$

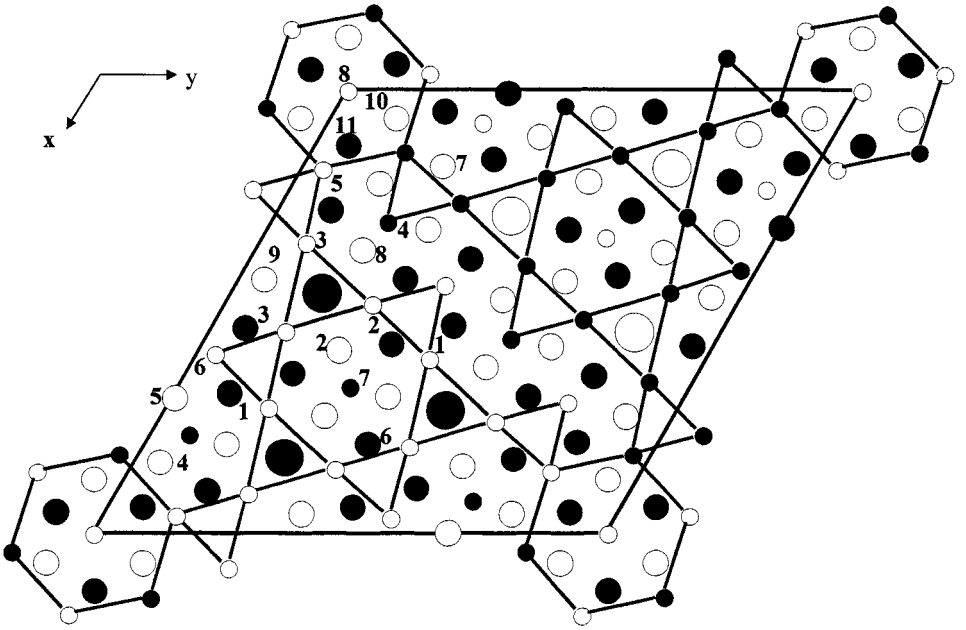

FIG. 1. Crystal structure of $Zr_6Cr_{60}P_{39}$ given in projection on the (001) plane. Large, medium and small circles represent zirconium, chromium, and phosphorus atoms, respectively. Full and open circles are translated from each other by half a period of the projection direction.

$R_{n(n-1)}T_{6(n^2+1)}X_{2(2n^2+1)+1}$ for the direct series. It can be noted that a similar formula has been proposed in the U–Mo–P system but no crystal data have been reported (19, 20). The general formula for the reverse series is $R_{n(n+1)}\square_{n(n-1)}T_{6(n^2+1)}X_{2(2n^2+1)+1}$. In both series $\square$ is a triangular metal vacancy, R holds for zirconium, rare earth element, or uranium in prismatic sites, T holds for a transition metal element in either pyramidal or tetrahedral sites, X is a metalloid atom, and n an integer. It is worth noting, from the above formulas, that the metal/metalloid ratio for the direct series $(R + T)/X = (7n^2 - n + 6)/(4n^2 + 3)$ is slightly lower than that of the reverse series

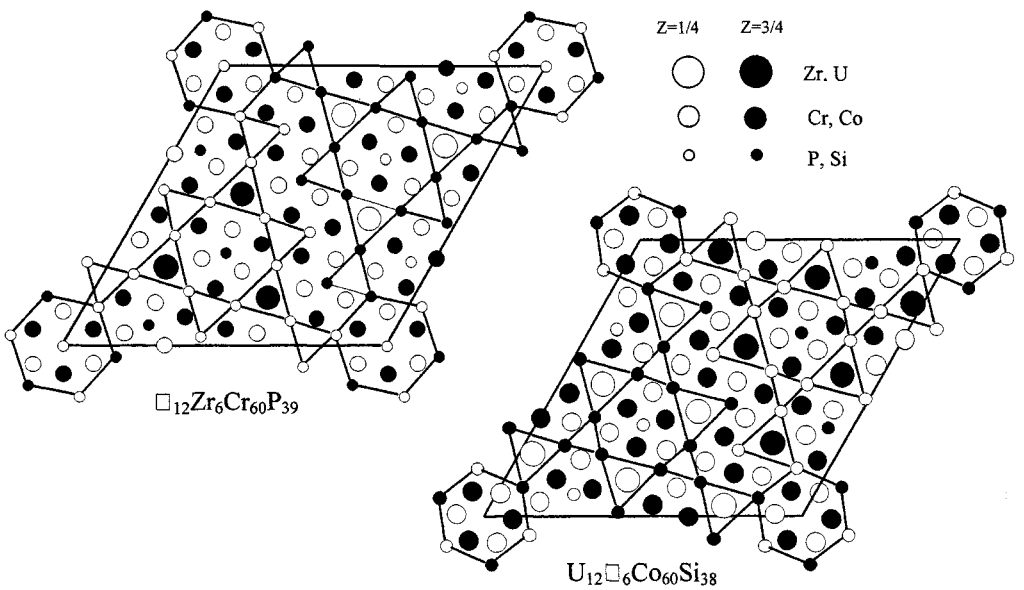

FIG. 2. Structural representations of $Zr_6Cr_{60}P_{39}$ and $U_{12}Co_{60}Si_{38}$ on the (001) plane. For comparison, the metalloïd network has been translated from $c/2$ between both structures.

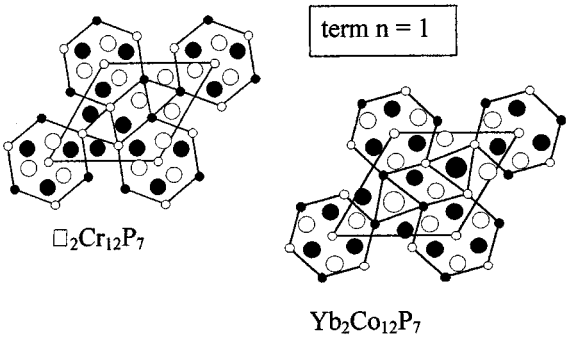
term n = 1
□2Cr12P7
Yb2Co12P7

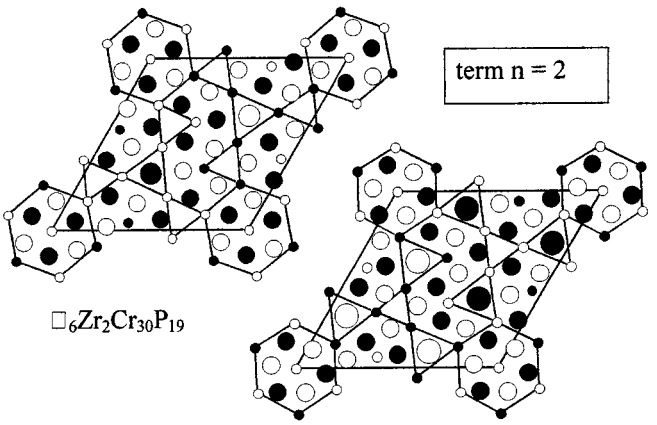
term n = 2
□6Zr2Cr30P19
Yb6□2Co30P19

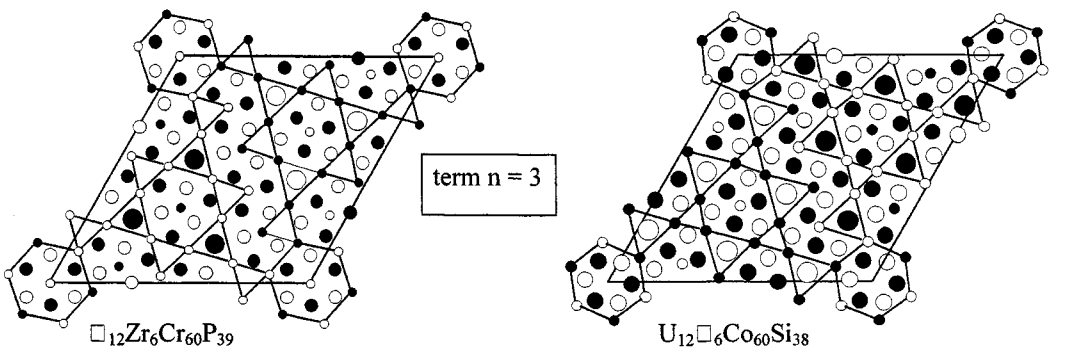
term n = 3
□12Zr6Cr60P39
U12□6Co60Si38

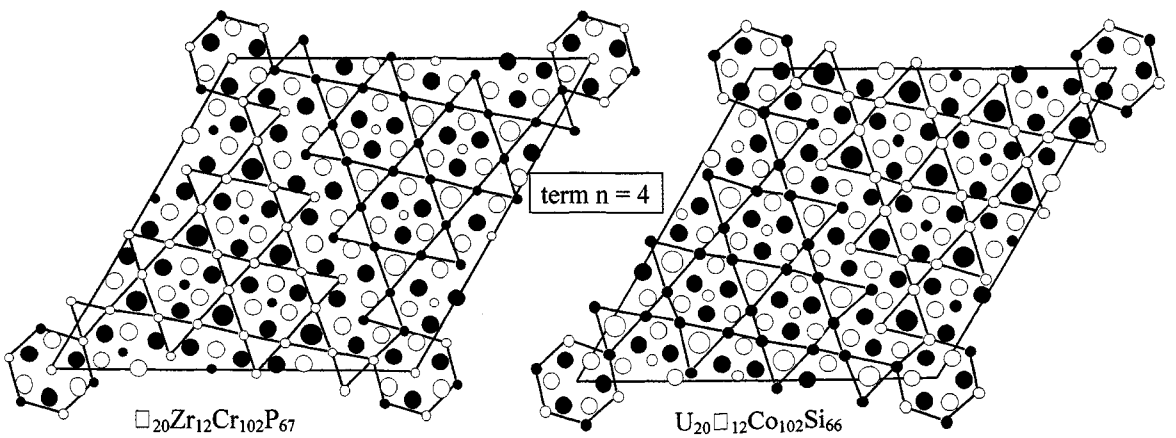
term n = 4
□20Zr12Cr102P67
U20□12Co102Si66

TABLE 4
Main Crystallographic Features [Unit Cell Parameters, Atomic Volume ($V_{at.}$)] and Number of Metalloid Polyhedra Occupied [prisms (pr), pyramids (py), tetrahedra (tet)] or Unoccupied [Triangles (tr)] by Metal Atoms for the Two Direct and Reverse Series

	Zr–Cr–P	Yb–Co–P	U–Co–Si
$n = 1$	$\square_2Cr_{12}P_7$ $a = 8.981$ Å, $V = 231.4$ Å^3 $c = 3.313$ Å, $V_{at.} = 12.18$ Å^3 2 *tr*, 9 *py*, 3 *tet*	$Yb_2Co_{12}P_7$ $a = 9.02$ Å, $V = 252.2$ Å^3 $c = 3.579$ Å, $V_{at.} = 12.00$ Å^3 2 *pr*, 9 *tet*, 3 *py*	$U_2Co_{12}Si_6$[a] $a \sim 8.49$ Å, $V \sim 230.3$ Å^3 $c \sim 3.69$ Å, $V_{at.} \sim 11.52$ Å^3 2 *pr*, 9 *tet*, 3 *py*
$n = 2$	$\square_6Zr_2Cr_{30}P_{19}$ $a = 14.807$ Å, $V = 635.4$ Å^3 $c = 3.348$ Å, $V_{at.} = 12.46$ Å^3 6 *tr*, 2 *pr*, 21 *py*, 9 *tet*	$Yb_6\square_2Co_{30}P_{19}$ $a = 14.703$ Å, $V = 669.1$ Å^3 $c = 3.578$ Å, $V_{at.} = 12.18$ Å^3 6 *pr*, 2 *tr*, 21 *tet*, 9 *py*	$U_6\square_2Co_{30}Si_{18}$ $a = 14.85$ Å, $V = 706.8$ Å^3 $c = 3.701$ Å, $V_{at.} = 13.09$ Å^3 6 *pr*, 2 *tr*, 21 *tet*, 9 *py*
$n = 3$	$\square_{12}Zr_6Cr_{60}P_{39}$ $a = 21.413$ Å, $V = 1332.3$ Å^3 $c = 3.354$ Å, $V_{at.} = 12.69$ Å^3 12 *tr*, 6 *pr*, 39 *py*, 21 *tet*		$U_{12}\square_6Co_{60}Si_{38}$ $a = 21.14$ Å, $V = 1429.2$ Å^3 $c = 3.693$ Å, $V_{at.} = 12.99$ Å^3 12 *pr*, 6 *tr*, 39 *tet*, 21 *py*
$n = 4$	$\square_{20}Zr_{12}Cr_{102}P_{67}$[a] $a \sim 27.50$ Å, $V \sim 2193.9$ Å^3 $c \sim 3.35$ Å, $V_{at.} \sim 12.12$ Å^3 20 *tr*, 12 *pr*, 63 *py*, 39 *tet*		$U_{20}\square_{12}Co_{102}Si_{66}$ $a = 27.53$ Å, $V = 2414.1$ Å^3 $c = 3.678$ Å, $V_{at.} = 12.84$ Å^3 20 *pr*, 12 *tr*, 63 *tet*, 39 *py*
$n = 5$	$\square_{30}Zr_{20}Cr_{156}P_{103}$[a] $a \sim 33.71$ Å, $V \sim 3296.7$ Å^3 $c \sim 3.35$ Å, $V_{at.} \sim 11.82$ Å^3 30 *tr*, 20 *pr*, 93 *py*, 63 *tet*		$U_{30}\square_{20}Co_{156}Si_{102}$[a] $a \sim 33.85$ Å, $V \sim 3661.5$ Å^3 $c \sim 3.69$ Å, $V_{at.} \sim 12.71$ Å^3 30 *pr*, 20 *tr*, 93 *tet*, 63 *py*

Note. For the U–Co–Si structure, owing to the absence of the silicon atom at the origin, there are in fact six truncated polyhedra (3 pyramids and 3 tetrahedra) around the *c* axis (see text).

[a]Crystallographic data for hypothetical compounds, not yet reported.

$(R + T)/X = (7n^2 + n + 6)/(4n^2 + 3)$). Moreover, the numbers of tetrahedral and pyramidal sites for the different members are easily derived from the formulas given above. Indeed, there are three tetrahedra for one prism and three pyramids for one triangular vacancy. Accordingly, there are $3n(n + 1)$ pyramids and $3n(n - 1)$ tetrahedra depending directly from prisms and triangles. When adding the three pyramids and the three tetrahedra of the hexagonal framework, the overall number becomes $3n(n + 1) + 3$ pyramids and $3n(n - 1) + 3$ tetrahedra for the direct series and *vice versa* for the reverse series.

The reasoning has been applied to the structures of $Cr_{12}P_7$, $Zr_2Cr_{30}P_{19}$, $Zr_6Cr_{60}P_{39}$ (direct series, members $n = 1$ to 3) and $R_2Co_{12}P_7$ (R = rare earth), $Yb_6Co_{30}P_{19}$ (or $U_6Co_{30}Si_{18+1}$), $U_{12}Co_{60}Si_{38+1}$, and $U_{20}Co_{102}Si_{66+1}$ (reverse series, members $n = 1$ to 4). The results are listed in Table 4 and the corresponding crystal structures are given in Fig. 3.

The member $n = 4$ of the reverse series $U_{20}Co_{102}Si_{66+1}$ has been reported by Aksel'rud *et al.* (21). It crystallizes in hexagonal symmetry with the unit cell parameters $a = 27.53(1)$ Å and $c = 3.678(1)$ Å. The structural features of $U_{20}Co_{102}Si_{66+1}$, previously compared with other uranium-containing silicides by Aksel'rud *et al.* (21), are summarized in Table 4. When comparing the unit cell parameters of the three silicides $U_6Co_{30}Si_{18+1}$, $U_{12}Co_{60}Si_{38+1}$, and $U_{20}Co_{102}Si_{66+1}$, it is worthwhile noting that the *a* parameter is a linear function of *n* (Fig. 4) while *c* remains quite constant. The same analysis applied to the direct series leads to extrapolation of the main features of the member $n = 4$, not yet reported. The predicted compound, with general formula $R_{12}T_{102}X_{67}$, more likely attainable in the Zr–Cr–P system as $Zr_{12}Cr_{102}P_{67}$, will have unit cell parameters $a \sim 27.50$ Å and $c \sim 3.35$ Å (Fig. 4). As mentioned before, the number of occupied and unoccupied metalloid polyhedra for the $Zr_{12}Cr_{102}P_{67}$ ternary phosph-

FIG. 3. Structural relationships between the members of the direct and the reverse series. Full and open circles are translated from each other by half a period of the projection direction. Large circles: Zr, U, Yb; medium circles: Cr, Co; small circles: P, Si.

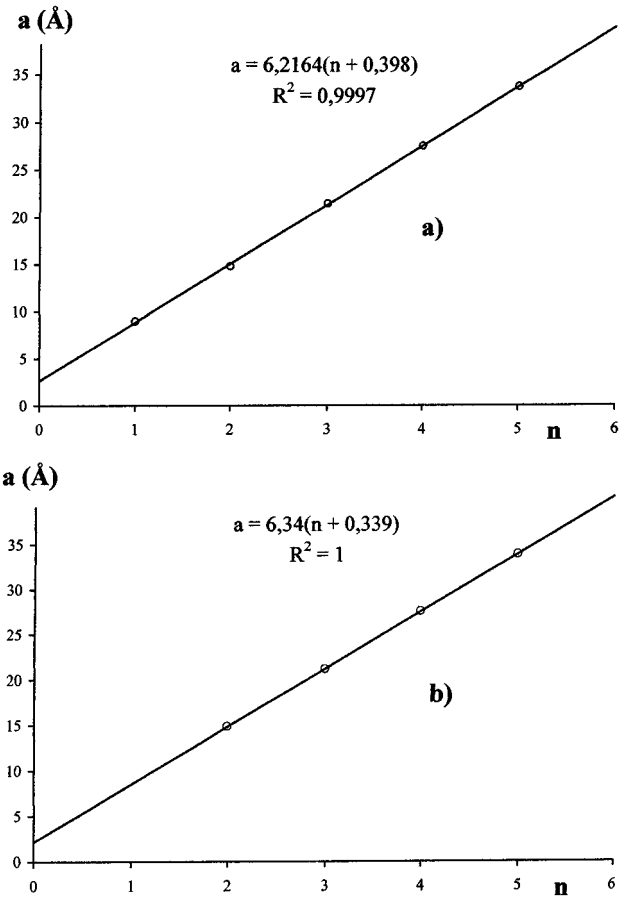

FIG. 4. Unit cell parameter a as a function of n in Zr–Cr–P (a) and U–Co–Si (b). The c values are almost constant for both series of compounds (see Table 4).

ide will be inverted compared with that observed for $U_{20}Co_{102}Si_{66+1}$. The main features (hexagonal unit cell parameters, formula, number of different polyhedra, positional parameters, etc.) for the not yet reported terms $n > 5$, for both direct and reverse series, can be deduced by the same arguments (Table 4).

The polyhedra size and interatomic distances previously reported for the Zr–Cr–P compounds, coupled with the criteria developed above, have been used to obtain the structural model (atomic coordinates not given here) of the ternary phase $Zr_{12}Cr_{102}P_{67}$ (Fig. 3). Its theoretical X-ray diffraction pattern, calculated using the program Fullprof (22) in the range $10^\circ \leq 2\theta \leq 70^\circ$ (isotropic thermal parameters of all atoms have been set to 0.5 Å^2) is compared in Fig. 5 with those of the other members of both series, calculated from their atomic positional coordinates as reported in the literature (1, 3–5, 17, 21). The visible differences between the X-ray diffraction patterns of $Zr_{12}Cr_{102}P_{67}$ and $U_{20}Co_{102}Si_{66}$ are similar to those observed for each n member for both series. One can see several reflections, with higher intensity roughly located before 35° (2θ) in the reverse series and a displacement for the strongest reflection toward low 2θ values of about 2° from direct to reverse series. Using these data, an accurate analysis of experimental X-ray powder diffraction patterns from syntheses in the Zr–Cr–P system has shown that the ternary $Zr_{12}Cr_{102}P_{67}$ was present in few samples as a minor phase with $Zr_6Cr_{60}P_{39}$. As can be seen in Fig. 5, the slight differences between the X-ray diffraction patterns within a given series explain why it was so difficult up to now, without the help of single crystals, to identify unambiguously the various phases from powder diffraction data.

Nevertheless, we recently proposed a general crystal chemical model to describe numerous intermetallics with M/X ratio equal or close to 2 (23). Besides the overall crystallographic features, we have shown that each phase can be identified easily on the basis of its strongest (hkl) reflection. Using this model, one can see that the strongest reflection, in the two series described herein, is (121) for member $n = 1$, (321) for member $n = 2$, (521) for member $n = 3$, and (721) for member $n = 4$ (Fig. 5). We note that the indexing of the strongest reflection identifies the member and that the series of defective compounds correspond to successive odd values of the h indexes, the other indexes (k, l) remaining constant. Therefore, the model provides a powerful tool to identify the different members of the series from X-ray powder diffraction data by using autoindexing programs and to perform Rietveld refinements.

At last, it is worth noting that the direct and reverse series are built from specific metal elements, i.e., from zirconium and chromium, on one hand, and from uranium and cobalt, on the other hand. The zirconium and uranium atoms (metallic radii of 1.60 and 1.54 Å, respectively) (16) occupy the largest available metalloid sites, i.e., the prisms. The main difference between the two series occurs from the 3d transition metal atoms (chromium and cobalt). According to Fruchart (24), the electronegativity and the size of the transition metal atoms govern the occupancy of pyramidal and tetrahedral metalloid sites in the family of M_2X compounds. The results we have obtained are in agreement with the conclusions of Fruchart. Indeed, the less electronegative and larger metal, here chromium, occupies preferentially the pyramidal sites, while the more electronegative and smaller metal, here cobalt, occupies the tetrahedral sites (see Table 4). Additional theoretical calculations would enable a better understanding of the occupancy or the nonoccupancy of the metalloid sites by metal atoms in the direct and reverse series.

CONCLUSION

The study of the Zr–Cr–P system led to the new structure type $Zr_6Cr_{60}P_{39}$ which belongs to the large family of M_2X

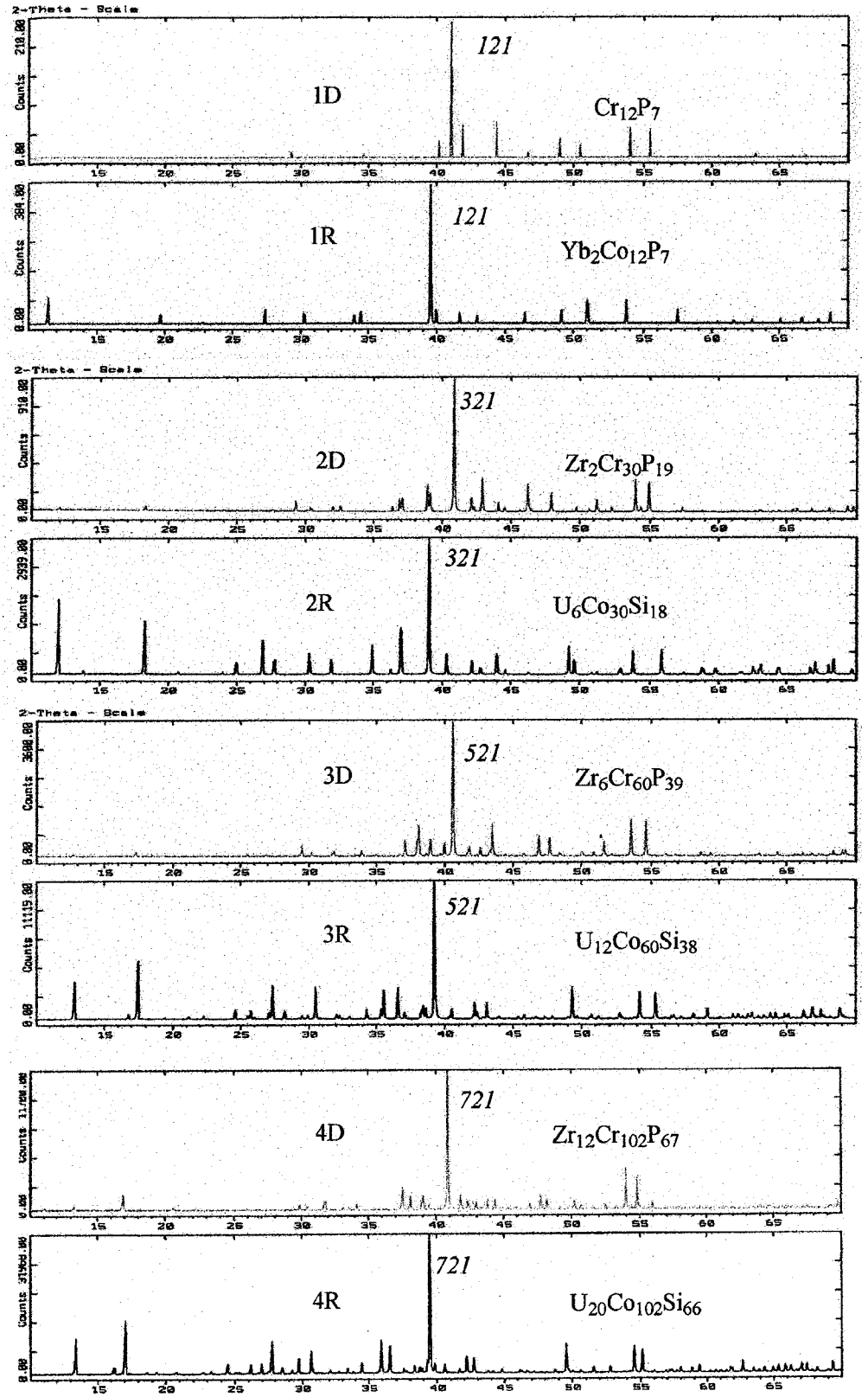

FIG. 5. X-ray diffraction patterns for members ($n = 1$ to 4) of the direct and reverse series. All patterns have been calculated by using the positional coordinates of compounds given in the literature, with the exception of that for $Zr_{12}Cr_{102}P_{67}$ (term $n = 4$ of direct series), which has been obtained from theoretical coodinates. Labeling 1D and 1R means term $n = 1$ of the direct (D) and reverse (R) series and so on.

and related intermetallic compounds. This new structure presents the usual coordination scheme: the zirconium atoms are in trigonal prismatic P coordination, while the chromium atoms occupy either pyramidal or tetrahedral phosphorus sites. Due to the occurrence of triangular phosphorus vacancies, the compound is metal defective and most of the phosphorus atoms exhibit a bicapped trigonal prismatic metal coordination. The structure of $Zr_6Cr_{60}P_{39}$ is closely related to that of the ternary silicide $U_{12}Co_{60}Si_{38}$ which has been described as a reverse structure. It has been shown that the structures of $Cr_{12}P_7$, $Zr_2Cr_{30}P_{19}$, and $Zr_6Cr_{60}P_{39}$, on one hand, and of $Yb_2Co_{12}P_7$, $Yb_6Co_{30}P_{19}$, $U_6Co_{30}Si_{18}$, $U_{12}Co_{60}Si_{38}$, and $U_{20}Co_{102}Si_{66}$, on the other hand, are members of two structural series respectively called direct and reverse series with the general formulas $\square_{n(n+1)}R_{n(n-1)}T_{6(n^2+1)}X_{2(2n^2+1)+1}$ (direct series) and $R_{n(n+1)}\square_{n(n-1)}T_{6(n^2+1)}X_{2(2n^2+1)+1}$ (reverse series). The structural relationships between the two series enable us to establish a general crystal chemical rule and to propose the theoretical crystal structure of the phosphide $Zr_{12}Cr_{102}P_{67}$ (member $n = 4$ of the direct series) without the help of single-crystal intensity data. In the same manner, the main crystallographic features of other members with $n > 5$, not yet reported in the literature, are proposed for the two series. The crystal chemical rule is therefore a powerful tool to count the occupied or unoccupied metalloid polyhedra, by metal atoms in the defective structures, and to obtain their theoretical X-ray diffraction patterns.

REFERENCES

1. C. Le Sénéchal, J. Y. Pivan, S. Députier, and R. Guérin, *Mater. Res. Bull.* **33,** 887 (1998).
2. W. Jeitschko and U. Jakubowski-Ripke, *Z. Kristallogr.* **207,** 69 (1993).
3. H. K. Chun and G. B. Carpenter, *Acta Crystallogr. Sect. B* **35,** 30 (1979).
4. W. Jeitschko, D. J. Braun, R. H. Ashcraft, and R. Marchand, *J. Solid State Chem.* **25,** 309 (1978).
5. Ya.P. Yarmolyuk, L. G. Aksel'rud, V. S. Fundamenskii, and E. I. Gladyshevskii, *Sov. Phys. Kristallogr.* **25,** 97 (1980).
6. N. F. M. Henry and K. Lonsdale (Eds.), "International Tables for Crystallography," Vol. I, 2nd ed. Kynoch Press, Birmingham, 1965.
7. C. K. Fair, "An Interactive Structure Solution Procedure", Enraf Nonius, Delft, 1990.
8. P. Main, S. J. Fiske, S. E. Hull, L. Lessinger, G. Germain, J. P. Declercq, and M. M. Woolfson, "MULTAN 11/82, A System of Computer Programs for the Automatic Solution of Crystal Structures from X-ray Diffraction Data," University of York/University of Louvain, 1982.
9. L. Pauling, *in* "Nature of the Chemical Bond," 3rd ed. Cornell Univ. Press, Ithaca, NY, 1960.
10. F. Hulliger and E. Mooser, *J Phys. Chem. Solids* **26,** 429 (1965).
11. J. Y. Pivan, R. Guérin, and M. Sergent, *J. Less-Common Met.* **107,** 249 (1985).
12. J. Y. Pivan and R. Guérin, *J. Less-Common Met.* **120,** 247 (1986).
13. J. Y. Pivan, R. Guérin, O. Pena, J. Padiou, and M. Sergent, *Mater. Res. Bull.* **23,** 513 (1988).
14. J. Y. Pivan, R. Guérin, O. Pena, J. Padiou, and M. Sergent, *Mater. Res. Bull.* **20,** 887 (1985).
15. S. Rundqvist and F. Jellinek, *Acta Chem. Scand.* **13,** 425 (1959).
16. F. Laves, *in* "Theory of Alloys Phases." ASM, Cleveland, OH, 1956.
17. Ya.P. Yarmolyuk, L.G. Aksel'rud, and E.I. Gladyshevskii, *Sov. Phys. Kristallogr.* **23,** 531 (1978).
18. E. Parthé, L. Gelato, B. Chabot, M. Penzo, K. Cenzual, and R. Gladyshevskii, *in* "Gmelin Handbook of Inorganic and Organometallic Chemistry," 8th ed. Springer-Verlag, Berlin, 1993.
19. R. Brink and W. Jeitschko, *Z. Kristallogr.* **182,** 46 (1988).
20. Yu.B. Kuz'ma and S. Chykhrij, *in* "Handbook on the Physics and Chemistry of Rare Earth" (K. A. Gschneidner, Jr., and L. Eyring, Eds.), Vol. 23, p. 285. Elsevier Science, Amsterdam, 1996.
21. L. G. Aksel'rud, Ya.P. Yarmolyuk, and E. I. Gladyshevskii, *Dop. Akad. Nauk Ukr. Rsr.* **42,** 79 (1980).
22. J. Rodriguez-Carvajal, *in* "Collected Abstracts of Powder Diffraction Meeting, Toulouse, 1990."
23. J. Y. Pivan and R. Guérin, *J. Solid State Chem.* **135,** 218 (1998).
24. R. Fruchart, *Ann. Chim. Fr.* **7,** 563 (1982).